Supporting Information

p-d Hybridization in CoFe LDH Nanoflowers for Efficient Oxygen Evolution Electrocatalysis

Liuyong Hu, [a#] Liliang Tian, [b#] Xiang Ding, [c#] Xia Wang, [a] Xiaosi Wang, [c] Ying Qin, [c] Wenling Gu, [c*] Le Shi, [b*] and Chengzhou Zhu [c*].

a Hubei Key Laboratory of Plasma Chemistry and Advanced Materials, Hubei Engineering Technology Research Center of Optoelectronic and New Energy Materials, Wuhan Institute of Technology, Wuhan 430205 (P. R. China)

b State key Laboratory of Electrical Insulation and Power Equipment, Center of Nanomaterials for Renewable Energy, School of Electrical Engineering, Xi'an Jiaotong University, Xi'an 710049 (P. R. China)

c Key Laboratory of Pesticide and Chemical Biology of Ministry of Education, International Joint Research Center for Intelligent Biosensing Technology and Health, College of Chemistry, Central China Normal University, Wuhan, 430079 (P. R. China)

*Corresponding author.

#These authors contributed equally.

E-mail addresses: wlgu@ccnu.edu.cn (Wenling Gu); le.shi@mail.xjtu.edu.cn (Le Shi); czzhu@ccnu.edu.cn (Chengzhou Zhu)

Table of contents

Experimental Section

Supporting Figures & Tables

Characterizations. Scanning electron microscopy (SEM) images were obtained from an XL30 ESEM FEG SEM (Philips, Netherlands). Transmission electron microscopy (TEM), high-resolution TEM (HR-TEM), high angle annular dark field-scanning TEM (HAADF-STEM) and elemental mapping were carried out on a TECNAI G2 HRTEM (Hitachi, Tokyo, Japan). X-ray photoelectron spectroscopy (XPS) was performed with an ESCALAB-MKII X-ray photoelectron spectroscopy (VG Scientific, UK). Powder X-ray diffraction (XRD) was conducted on a D8 ADVANCE (Germany) using Cu Kα radiation (λ =1.5406 Å). Fourier transform infrared (FTIR) spectrum was characterized by a TENSOR27 (Bruker, United States). Linear sweep voltammetry (LSV), cyclic voltammetric (CV) and amperometric *i-t* curves were measured with a CH Instruments 660D voltammetric analyzer.

Electrochemical Measurements. The electrochemical activity was evaluated by a CHI 660E electrochemical workstation (CH Instruments, Shanghai) with a standard three-electrode system. The polished graphite rod and saturated calomel electrode (SCE) were used as a counter electrode and a reference electrode, respectively, while the NF was supported with MIM-CoFe LDH catalyst as the working electrode. In addition, the CoFe LDH, pristine NF and RuO_2 catalyst were also characterized for comparisons. The measured potentials in this work were converted to the reversible hydrogen electrode (RHE) according to the formula of E (*vs*. RHE) = E (*vs*. SCE) + 0.241 + 0.059 pH. The linear sweep voltammetry (LSV) measurements were performed in O_2-saturated 1.0 M KOH electrolyte with the scan rate of 2 mV/s to evaluate the OER activity of prepared catalysts. All the potential in LSV curves were

corrected for *iR* losses. Electrochemical impedance spectroscopy (EIS) measurement were carried out with 5 mV amplitude with a frequency range from 10^5 to 1 Hz at 1.45 V vs. RHE. Furthermore, the amperometric *i-t* curves were acquired by sweeping the MIM-CoFe LDH/NF with 24 h in O_2-saturated 1.0 M KOH solution. The turnover frequency (TOF) was calculated by the equation: TOF = (J×A) / (4×F×m), where J represents the current density (A cm^{-2}) at an overpotential of 300 mV, A and m represent the area of the electrode and the number of moles of the active materials. The Faradaic efficiency was calculated as follows: $F_r = |I_r n_d / I_d n_r N_{CL}|$, where I_r is the ring current, I_d, is the disk current, n_d and n_r are the electron transfer number of the reaction on disk ($4OH^- \rightarrow 4e^- + 2H_2O + O_2$) and ring ($2H_2O + O_2 + 2e^- \rightarrow 2OH^- + H_2O_2$), respectively. Moreover, the N_{CL} (N_{CL} = 0.37) is the collect efficiency.

Computational Methods. Theoretical computations were performed using CP2K software package[1], which is based on the density function theory (DFT) framework under periodic boundary conditions. Using the Gaussian and plane-wave methods, the wave function was expanded in the Gaussian double zeta with valence polarization (DZVP) function basis set. The core electrons were treated using PBE gradient correction[2] and Goedecker−Teter−Hutter (GTH) pseudopotentials[3]. A plane-wave energy cut-off of 400 Ry has been employed. Density functional theory (DFT)-D3 correction[4] was used to account for the van der Waals interaction. The Monkhorst−Pack k-point mesh was set to be <0.05 $Å^{-1}$ and a vacuum space of 2 nm in the *z*-direction was added to avoid interactions between periodic images.

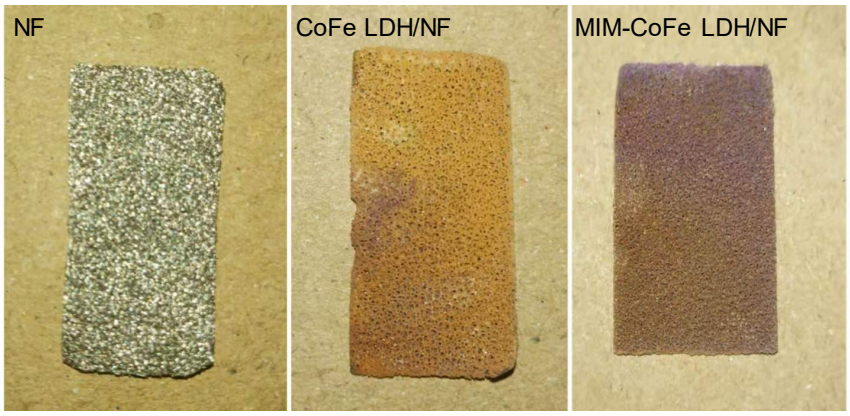

Fig. S1. Digital images of NF, CoFe LDH/NF and MIM-CoFe LDH/NF.

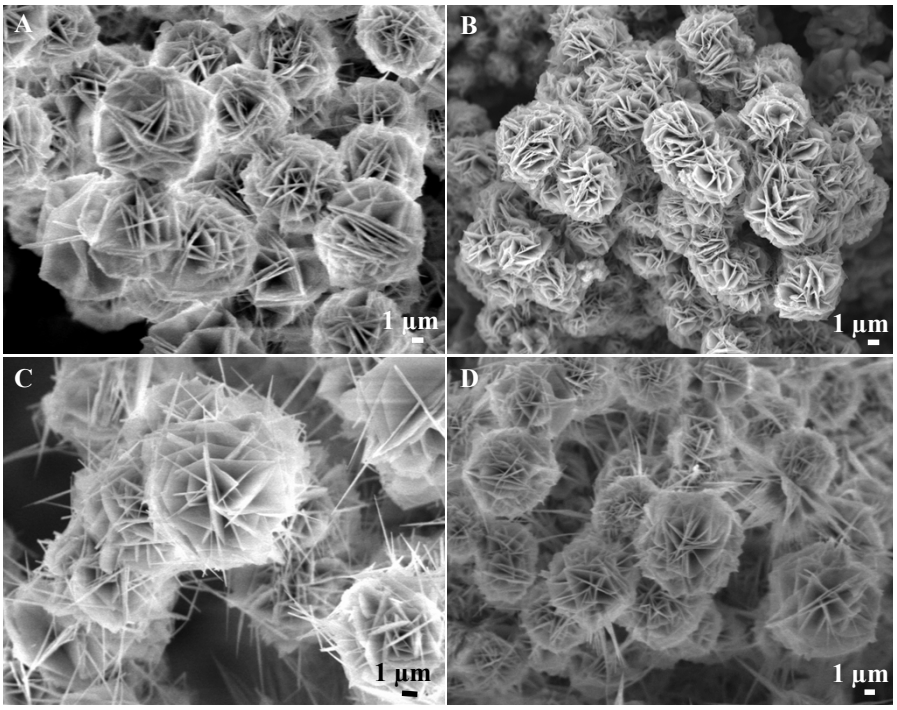

Fig. S2. SEM images of CoFe LDH/NF (A), MIM-CoFe LDH/NF-5 min (B), MIM-CoFe LDH/NF-30 min (C), and MIM-CoFe LDH/NF-120 min (D).

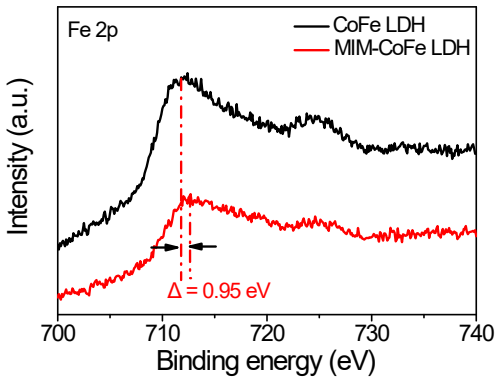

Fig. S3. High-resolution Fe 2p XPS peaks of as-prepared CoFe LDH and MIM-CoFe LDH.

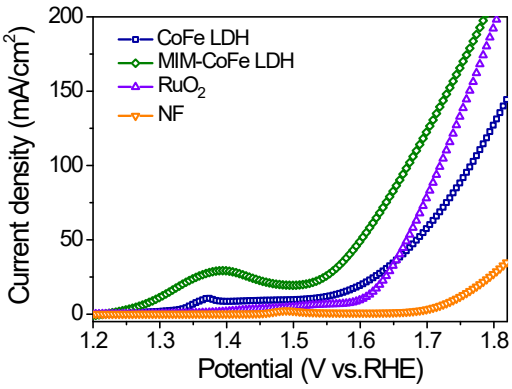

Fig. S4. OER polarization curves of the samples without iR correction.

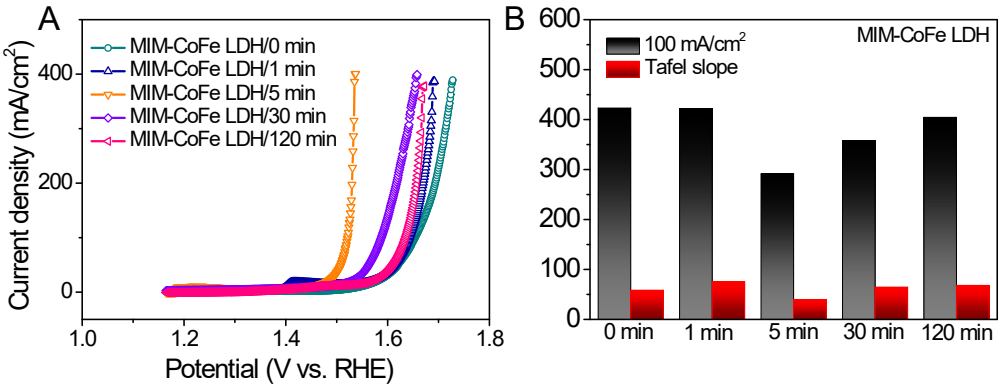

Fig. S5. OER polarization curves (A) and overpotentials at j = 100 mA/cm^2 and Tafel slopes (B) of CoFe LDH and MIM-CoFe LDH with different reaction times.

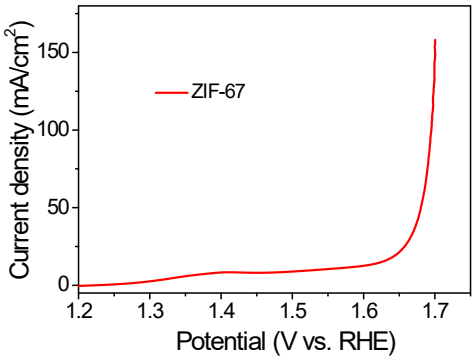

Fig. S6. OER polarization curve of ZIF-67.

Fig. S7. CV curves of MIM-CoFe LDH (A) and CoFe LDH (B) at different scan rates.

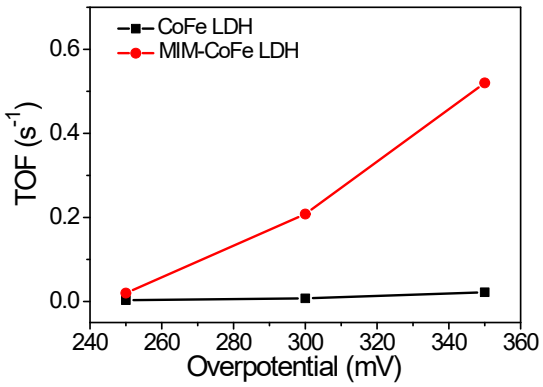

Fig. S8. TOF values of MIM-CoFe LDH and CoFe LDH at different overpotentials.

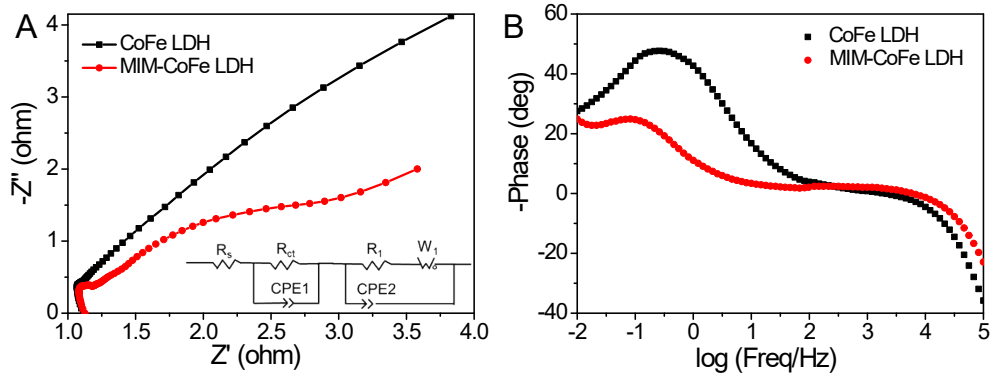

Fig. S9. Nyquist (A) and Bode (B) plots of MIM-CoFe LDH and CoFe LDH.

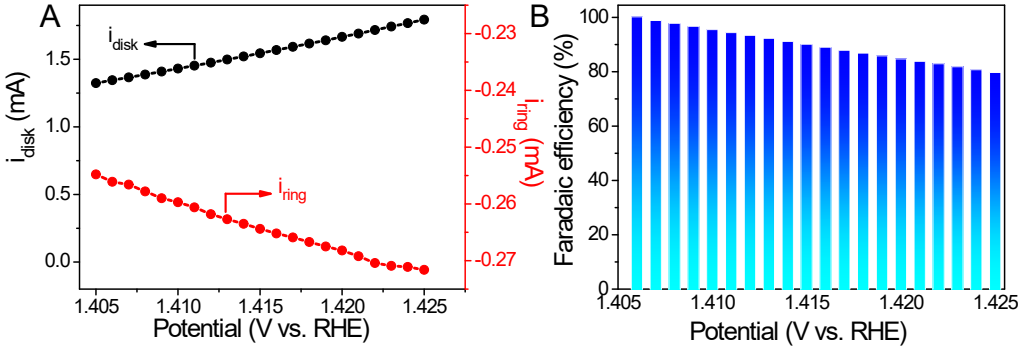

Fig. S10. (a) Disk and ring current of MIM-CoFe LDH tested on RRDE in a 1.0 M KOH solution with a ring potential of 0.4 V. (b) Faradaic efficiency of the catalyst in 1.0 M KOH at 1600 rpm under N_2 saturation.

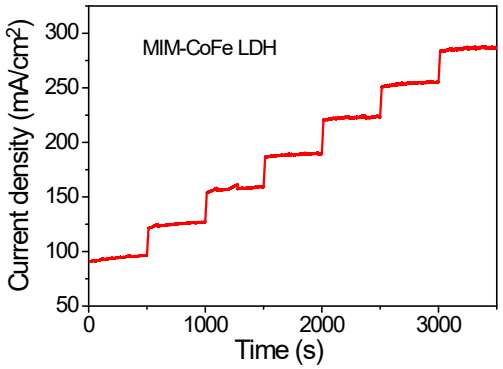

Fig. S11. Multicurrent process curve of MIM-CoFe LDH.

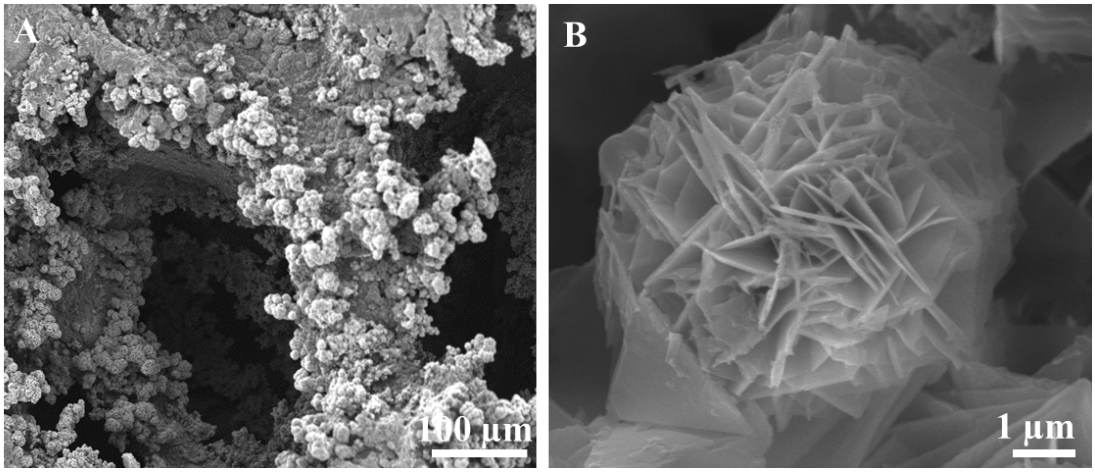

Fig. S12. SEM images of MIM-CoFe LDH after stability test.

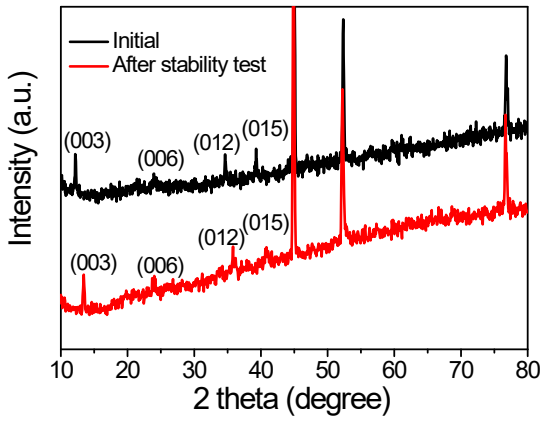

Fig. S13. XRD patterns of MIM-CoFe LDH before and after stability test.

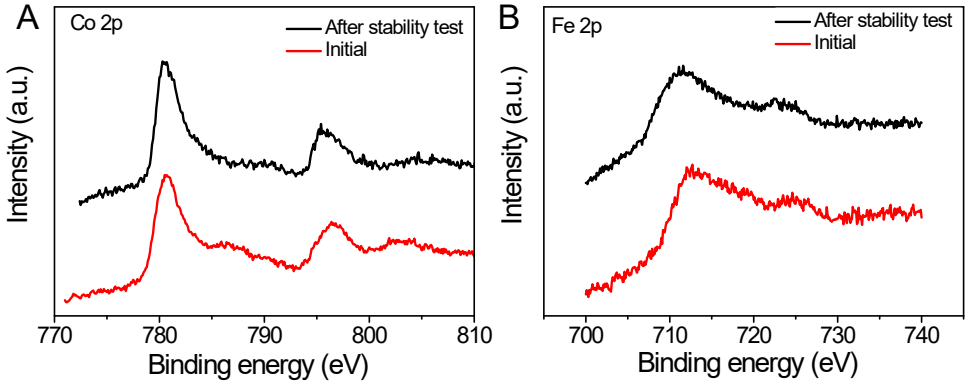

Fig. S14. XPS results of MIM-CoFe LDH before and after stability test.

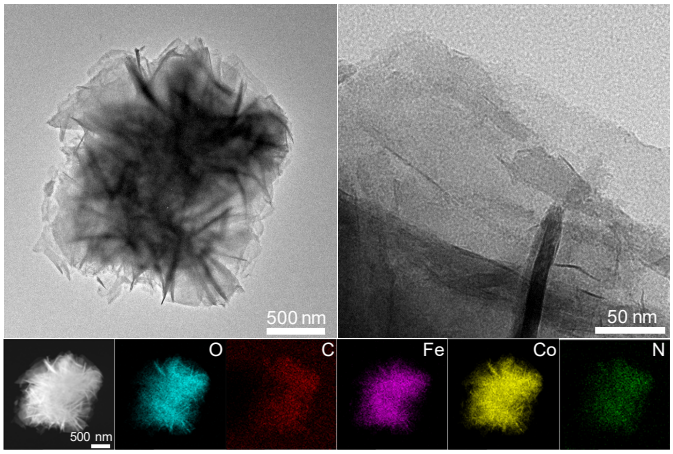

Fig. S15. HRTEM and EDX elemental mapping images of MIM-CoFe LDH after stability test.

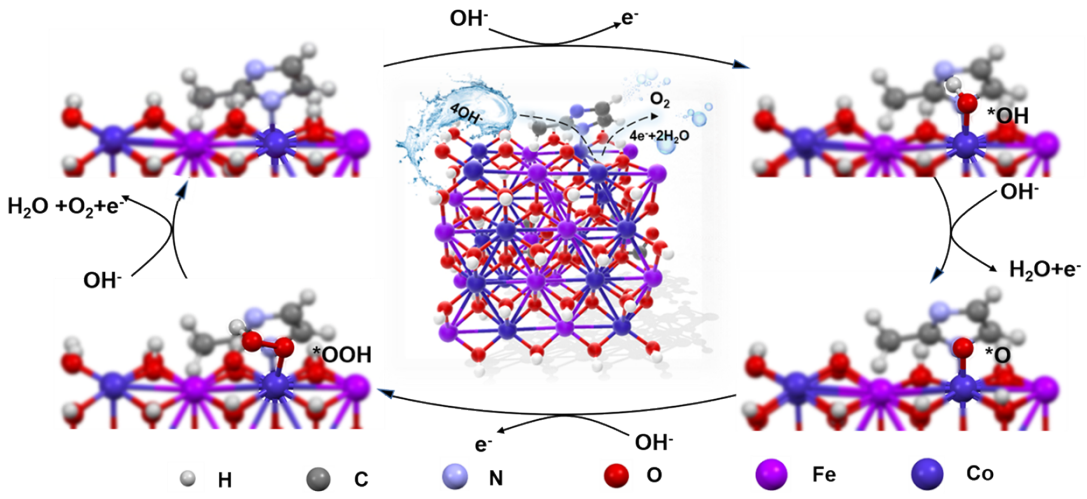

Fig. S16. Mechanism of OER on MIM-CoFe LDH.

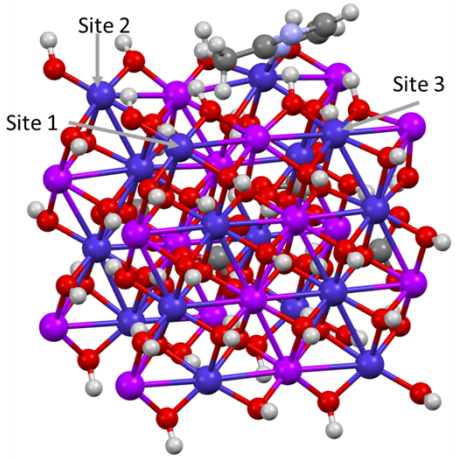

Fig. S17. Considered reaction sites of MIM-CoFe LDH for the OER process.

Table S1. Gibbs free energy changes during OER process taken place at the different reaction sites.

Adsorption site	ΔG1 (eV)	ΔG2 (eV)	ΔG3 (eV)	ΔG4 (eV)	η (eV)
CoFe LDH site1	-0.256	1.748	1.356	2.072	0.842
MIM-CoFe LDH site1	0.003	1.519	1.625	1.774	0.544
MIM-CoFe LDH site2	-0.559	1.679	1.278	2.522	1.292
MIM-CoFe LDH site3	-0.233	1.621	1.094	2.438	1.208

References

(1) VandeVondele, J.; Krack, M.; Mohamed, F.; Parrinello, M.; Chassaing, T.; Hutter, J. QUICKSTEP: Fast and Accurate Density Functional Calculations Using a Mixed Gaussian and Plane Waves Approach. *Comput. Phys. Commun.* **2005**, *167*, 103-128.

(2) Perdew, J. P.; Ernzerhof, M.; Burke, K. Rationale for Mixing Exact Exchange with Density Functional Approximations. *J. Chem. Phys.* **1996**, *105*, 9982-9985.

(3) Goedecker, S.; Teter, M.; Hutter, J. Separable Dual-Space Gaussian Pseudopotentials. *Phys. Rev. B* **1996**, *54*, 1703-1710.

(4) Grimme, S.; Antony, J.; Ehrlich, S.; Krieg, H. A Consistent and Accurate Ab Initio Parametrization of Density Functional Dispersion Correction (DFT-D) for the 94 Elements H-Pu. *J. Chem. Phys.* **2010**, *132*, 154104.